The Astrophysical Journal, 648:753–761, 2006 September 1
Copyright is not claimed for this article. Printed in U.S.A.

TEMPERATURE DEPENDENCE OF THE FORMATION OF HYDROGEN, OXYGEN, AND HYDROGEN PEROXIDE IN ELECTRON-IRRADIATED CRYSTALLINE WATER ICE

Weijun Zheng,[1,2] David Jewitt,[1] and Ralf I. Kaiser[2]
Received 2005 December 15; accepted 2006 May 16

ABSTRACT

We conducted a systematic study of the irradiation of crystalline water ice in an ultrahigh vacuum chamber at pressures of about 10^{-10} torr. Crystalline water ices of 115 ± 30 nm thickness were irradiated with energetic electrons at 12, 40, 60, and 90 K to simulate energetic particle interaction with solar system and interstellar water ices. The production rates of molecular hydrogen (H_2), molecular oxygen (O_2), and hydrogen peroxide (H_2O_2) decrease as the temperature rises from 12 to 90 K. These findings strongly indicate a thermal, possibly diffusion-controlled component of the reaction mechanism, which could facilitate the back-reaction of the primarily formed irradiation products such as the recombination of atomic hydrogen (H) with the hydroxyl radical (OH) to "recycle" water. This study underlines the necessity to provide temperature-dependent rate constants on the formation of molecules in planetary and interstellar ices and to include nonequilibrium as well as thermal chemistry in reaction models simulating the chemical processing of extraterrestrial ices. We estimate the concentrations of newly formed H_2O_2 molecules in the irradiated water ice at 90 K to be in the same order of magnitude as the concentration of H_2O_2 observed on the Galilean satellites.

Subject headings: astrobiology — astrochemistry — comets: general — cosmic rays — infrared: ISM — ISM: clouds — ISM: molecules — methods: laboratory — molecular processes

1. INTRODUCTION

Water ice is abundant in both molecular clouds and planetary systems (Brown & Cruikshank 1997; Greenberg et al. 1983). Kuiper Belt objects (Jewitt & Luu 1993), satellites in the outer solar system like Europa and Ganymede (Calvin et al. 1995), the nuclei of comets (Davies et al. 1997; Festou et al. 2004), and some planetary rings (Sicardy 2005) are all known to be water-rich. The icy dust grains in molecular clouds are subject to irradiation by the Galactic cosmic-ray particles (Cesarsky & Volk 1978; Clayton & Jin 1995) and by ultraviolet (UV) photons from the internal photon field (Cecchi-Pestellini et al. 1995). Kuiper Belt objects are chemically processed by Galactic cosmic-ray particles, UV photons, and the solar wind (Cooper et al. 2003). The icy satellites in the outer solar system are—in addition to the previously mentioned high-energy sources—also bombarded by energetic particles trapped in planetary magnetospheres (Cooper et al. 2001). Therefore, the processing of water ices by energetic particles and UV photons plays an important role in astrochemistry and in the chemical evolution of the solar system. The temperatures of water ice in the interstellar and planetary environments are quite different. Water-rich interstellar grains in cold molecular clouds have temperatures near 10 K (Kruegel & Walmsley 1984), whereas the temperatures of Kuiper Belt objects, Saturn's rings, and the Jovian satellites have been estimated to be about 50 K (Jewitt & Luu 2004), 70–110 K (Flasar et al. 2005; Hanel et al. 1982), and 80–150 K (Hanel et al. 1979; Spencer et al. 1999), respectively. Since the rates of chemical reactions, diffusion coefficients, and the underlying chemical dynamics can depend strongly on the temperature (Kaiser 2002), we expect that the temperatures in extraterrestrial solids will also have a profound effect on the chemical processing of the water-rich ices. Therefore, an investigation of the irradiation of water ice at different temperatures is very important for the understanding of the chemical processing of interstellar and solar system objects.

The irradiation and sputtering effects on water ice at different temperatures have been studied extensively in laboratory experiments (Baragiola 2003; Johnson et al. 2005; Johnson & Quickenden 1997; Loeffler & Baragiola 2005, and references therein) during the last quarter of a century. Moore & Hudson (2000) investigated the formation of hydrogen peroxide (H_2O_2) in water ice by proton (0.8 MeV) irradiation at 16 and 80 K. Although H_2O_2 was detected by infrared (IR) absorption spectroscopy at 16 K, it was undetectable at 80 K. Gomis et al. (2004a) studied the irradiation of water ice with H^+ (200 keV), He^+ (200 keV), and Ar^{++} (400 keV) at 16 and 77 K. In contrast to Moore & Hudson (2000), these authors observed the formation of H_2O_2 via IR transmission spectroscopy at both temperatures. Bahr et al. (2001) monitored the temperature-dependent formation of molecular oxygen (O_2) and H_2O_2 with a quadrupole mass spectrometer released from cubic water ices irradiated with 200 keV protons between 40 and 120 K. These preliminary studies show the influence of temperature on the production rates of molecules in water ices on high-energy processing. However, despite the importance of these processes, no systematic, mechanistic studies on the production rates of astrochemically important molecules like molecular hydrogen and oxygen, as well as hydrogen peroxide, have been reported to date.

In our previous work, we reported the formation of H_2, O_2, and H_2O_2 in crystalline water ice by electron irradiation at 12 K (Zheng et al. 2006). Here, we expand these investigations to elucidate the temperature-dependent production rates of those species at 12, 40, 60, and 90 K. The experimental results are then compared to the concentration of hydrogen peroxide as observed on Jupiter's inner satellites (Carlson et al. 1999; Hendrix et al. 1999).

2. EXPERIMENTAL

The experiments were carried out in a contamination-free ultrahigh vacuum chamber ($<10^{-10}$ torr), which has been introduced

[1] Institute for Astronomy, University of Hawaii at Manoa, Honolulu, HI 96822.
[2] Department of Chemistry, University of Hawaii at Manoa, Honolulu, HI 96822; kaiser@gold.chem.hawaii.edu.

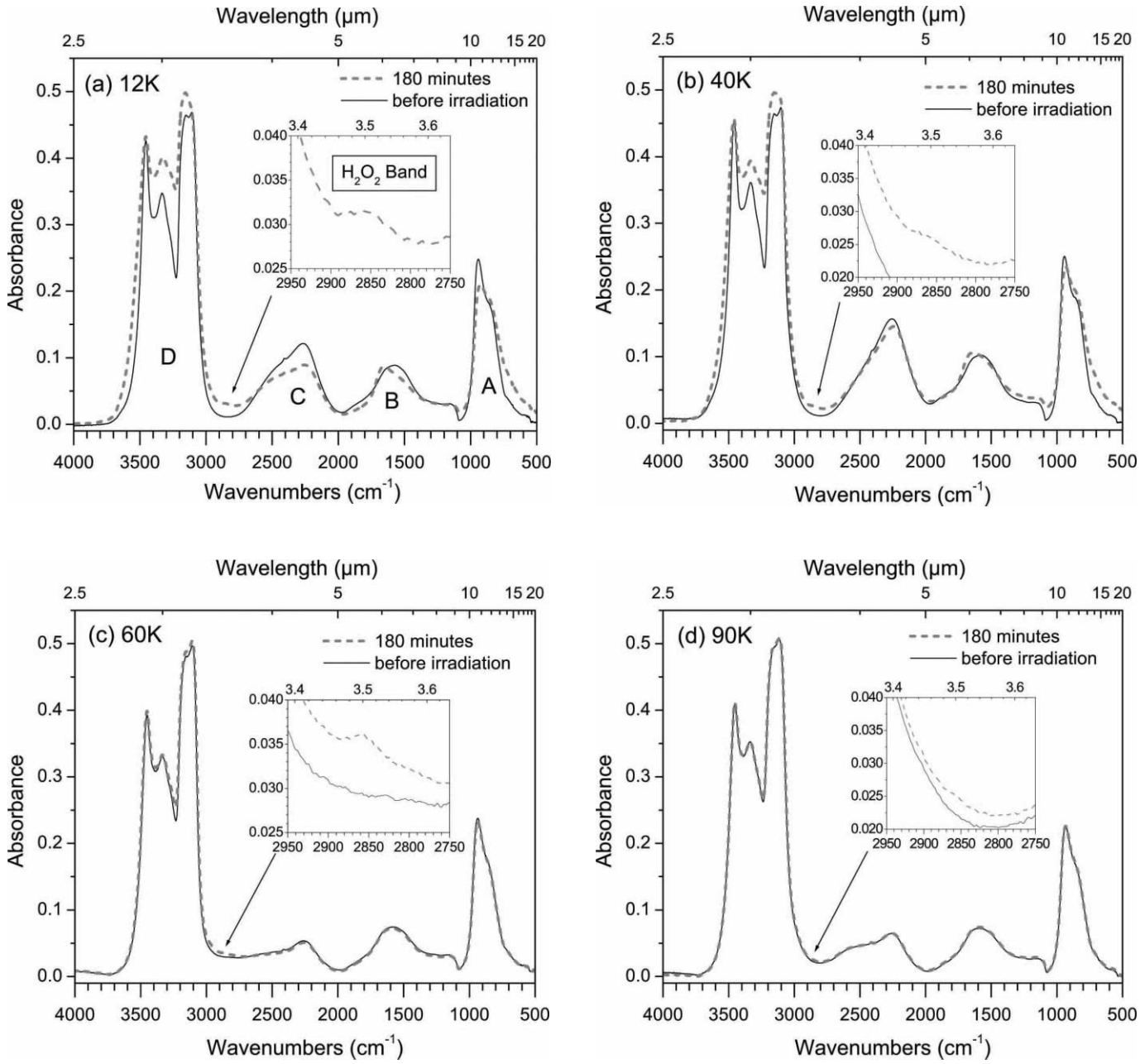

FIG. 1.—Typical IR spectra of water ice before and after irradiation with 5 keV electrons at 1000 nA current.

elsewhere (Bennett et al. 2004; Zheng et al. 2006). Briefly, a two-stage closed-cycle helium refrigerator coupled with a rotary platform is attached to the main chamber and holds a polished polycrystalline silver mirror serving as a substrate for the ice condensation. With the combination of the closed-cycle helium refrigerator and a programmable temperature controller, the temperature of the silver mirror can be regulated precisely (±0.3 K) between 10 and 350 K. A valve and a glass capillary array are used to condense gases on the silver mirror. The actual thickness of the ice samples can be controlled via the condensation time and the water partial pressure in the main chamber. Crystalline water ice samples of 115 ± 30 nm thickness were prepared by condensing water vapor onto the silver substrate at 140 K (Zheng et al. 2006). To minimize the contamination from air inside the water ice, we froze triply distilled water with liquid nitrogen and repeatedly defrosted it in vacuum. The gas reservoir was pumped down to 10^{-7} torr before it was filled with about 11 torr water vapor. During the deposition, the water vapor pressure in the main chamber was maintained at 6×10^{-9} torr for 9 minutes. The samples were cooled down slowly to the desired temperatures (12, 40, 60, and 90 K) with a cooling rate of 1.0 K minute^{-1}. They were then irradiated with 5 keV electrons for 180 minutes at beam currents of 0 (blank experiment), 10, 100, 1000, and 10,000 nA by scanning the electron beam over an area of 1.86 ± 0.02 cm^2. We demonstrated earlier that these 5 keV electrons can mimic efficiently the chemical processing of interstellar water-rich ices by energetic electrons generated in the track of cosmic-ray particles (Bennett et al. 2004, 2005; Jamieson et al. 2005). After each irradiation, the sample was kept at the same temperature for 60 minutes and then warmed up at 0.5 K minute^{-1} to 293 K. The IR spectra of the samples were measured online and in situ by a Fourier transform IR spectrometer (Nicolet 510 DX

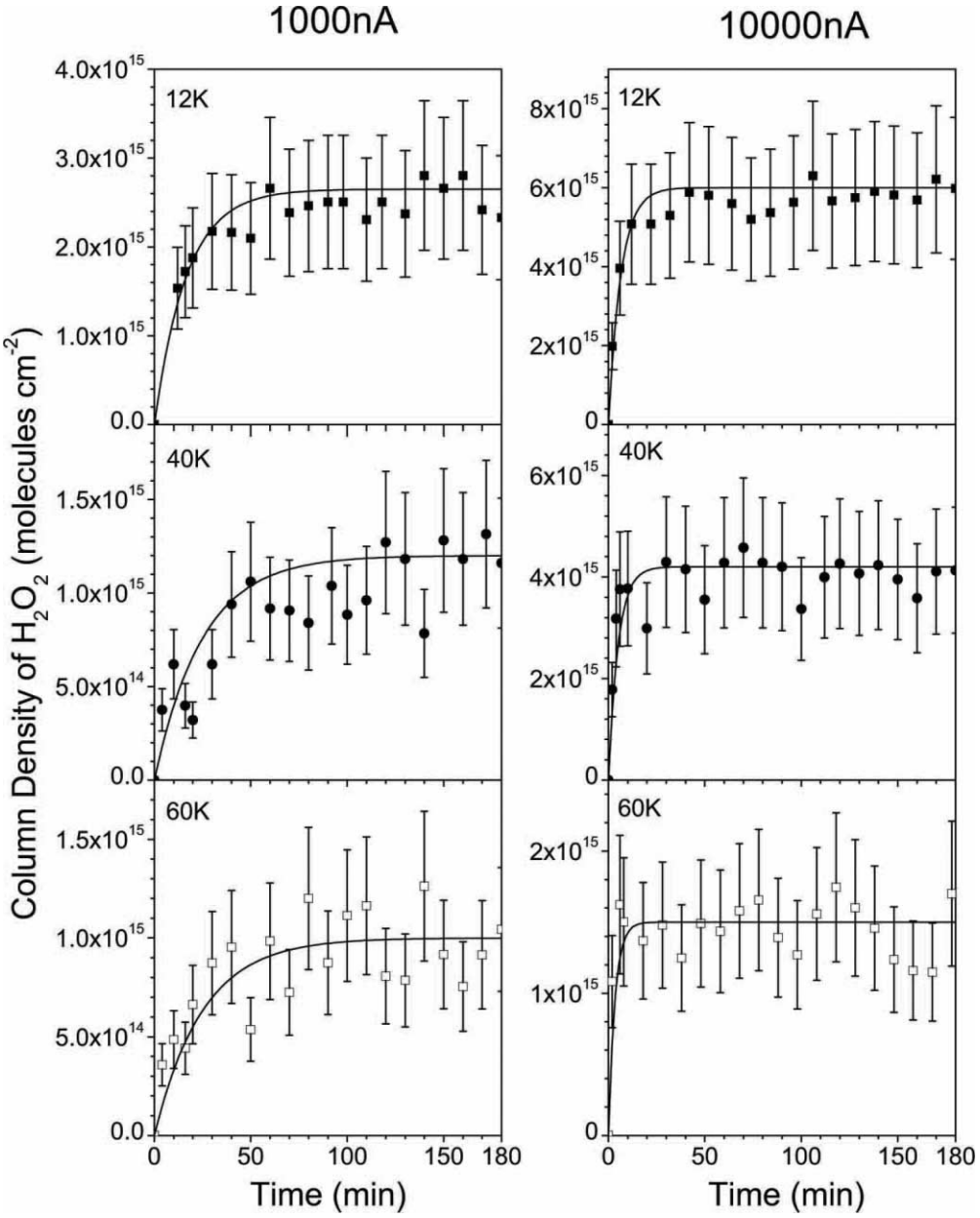

FIG. 2.—Temporal evolution of the H_2O_2 column density during the irradiation exposure at electron currents of 1000 and 10,000 nA. The solid lines present the best fits. The water ice temperatures (12, 40, and 60 K) are labeled in the graphs.

FTIR); the species subliming from the samples were monitored with a quadrupole mass spectrometer (Balzer QMG 420).

3. RESULTS

3.1. *Infrared Spectra*

In Figure 1, the IR spectra before (*solid lines*) and after (*dashed lines*) the irradiation are shown at four temperatures. In the IR spectra of cubic crystalline water ice, the absorption bands centered at 941 and 1574 cm^{-1} correspond to the libration band (ν_L) and bending mode (ν_2), respectively. The absorption band centered at 2270 cm^{-1} results from a combination of bands ($\nu_L + \nu_2$) or libration overtone ($3\nu_L$). The bands at 3107 and 3452 cm^{-1} correspond to the in-phase and out-of-phase symmetric stretch (ν_1); those at 3151 and 3332 cm^{-1} are from the transversal and longitudinal modes of the asymmetric stretch (ν_3). The irradiation induced several major changes in the spectrum of crystalline water ice. From the chemical viewpoint, hydrogen peroxide (H_2O_2) is the only newly formed molecule detected via its absorption at 2850 cm^{-1}. This feature has been discussed previously (Baragiola et al. 2005; Moore & Hudson 2000). Most important, as the temperature increases during the irradiation experiment from 12 (Fig. 1*a*) to 90 K (Fig. 1*d*), the intensity of this absorption decreases. We also monitored a change in the line profiles with increasing irradiation time. Here, the absorption feature A (Fig. 1) became less intense and broadened, feature B showed a blueshift, the intensity of absorption C dropped, and feature D also broadened after the irradiation. Most important, the intensity in the center of feature D increased significantly. As we discussed in a previous paper (Zheng et al. 2006), there are also prominent hydrogen peroxide absorption bands at 3175 (ν_5) and 3285 cm^{-1} (ν_1). Hence, the hydrogen peroxide might also contribute to the change in feature D. The overall spectral changes resulting from the irradiation become smaller as the temperature increases from 12 to

TABLE 1

PARAMETERS OF THE TEMPORAL EVOLUTION FOR THE H_2O_2 COLUMN DENSITIES MEASURED FROM THE 2850 cm^{-1} (3.5 μm) ABSORPTION BAND

	1000 nA		10,000 nA	
TEMPERATURE (K)	a (molecules cm^{-1})	k ($minutes^{-1}$)	a (molecules cm^{-1})	K ($minutes^{-1}$)
12	$2.7 \pm 0.8 \times 10^{15}$	0.06 ± 0.02	$6.0 \pm 1.8 \times 10^{15}$	0.16 ± 0.05
40	$1.2 \pm 0.4 \times 10^{15}$	0.04 ± 0.02	$4.2 \pm 1.4 \times 10^{15}$	0.20 ± 0.07
60	$1.0 \pm 0.4 \times 10^{15}$	0.04 ± 0.02	$1.5 \pm 0.5 \times 10^{15}$	0.30 ± 0.10

90 K (Fig. 1). At 90 K, the spectra before and after the irradiation are almost identical.

We were also able to monitor the H_2O_2 column density during the irradiation via the intensity of its 2850 cm^{-1} (3.5 μm) absorption band. The intensities of the H_2O_2 absorption band (2850 cm^{-1}) at different temperatures show that the production rates of H_2O_2 decrease as the temperature rises from 12 to 90 K. Figure 2 presents the temporal evolution of the H_2O_2 column density fitted via pseudo-first-order kinetics through equation (1):

$$n(t) = a\left(1 - e^{-kt}\right), \quad (1)$$

where t is the irradiation time, $n(t)$ is the column density of H_2O_2 molecules generated by irradiation, and a and k are constants. The parameters of the fits are shown in Table 1. The H_2O_2 column density at 90 K is too low to measure accurately, and its temporal evolution is not shown here.

3.2. *Mass Spectra*

Figure 3 shows the ion currents of molecular hydrogen at mass-to-charge (m/z) of $m/z = 2$, molecular oxygen ($m/z = 32$), water ($m/z = 18$), and hydrogen peroxide ($m/z = 34$) released into the gas phase during warming up. Figures 3*a*–3*d* correspond

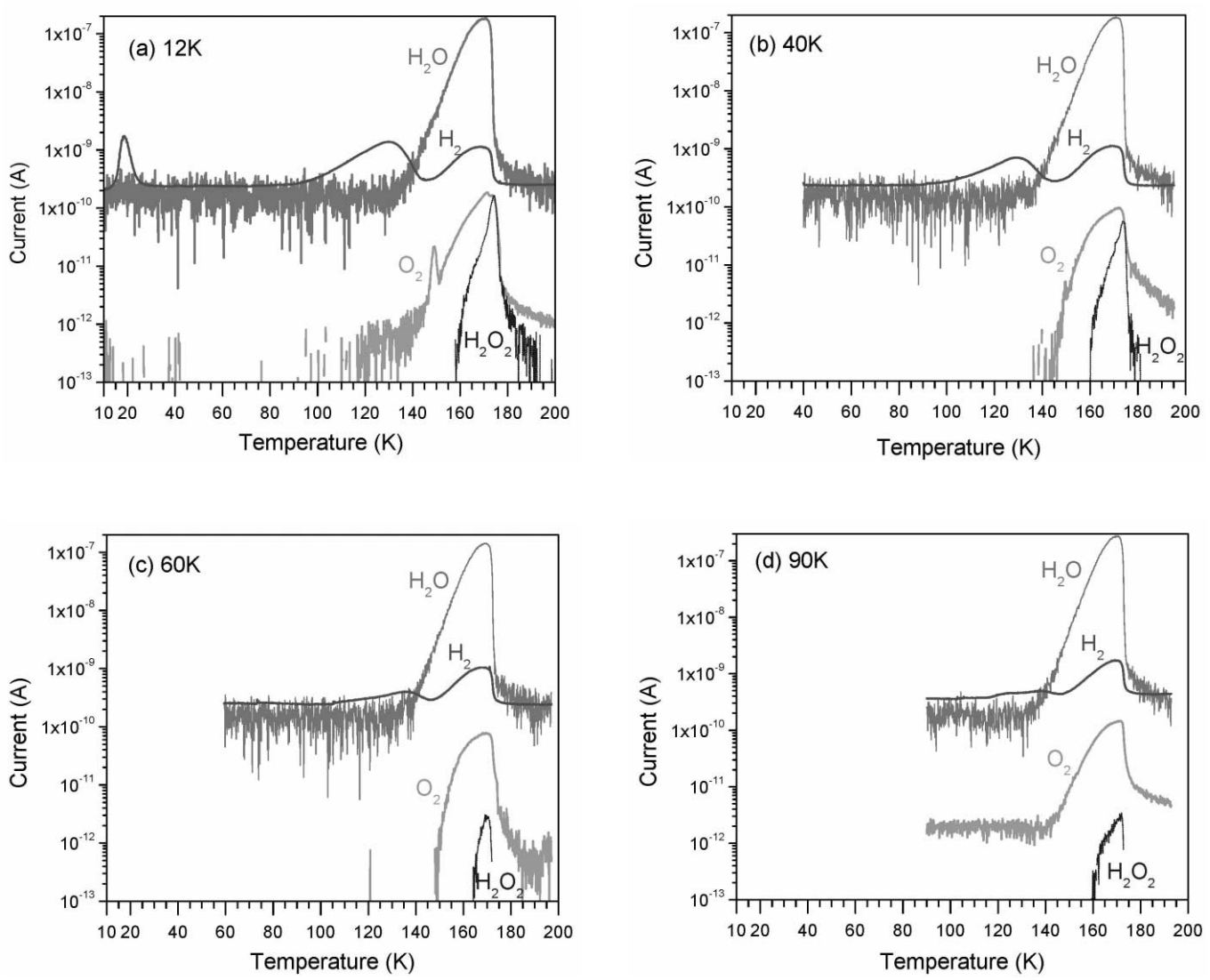

FIG. 3.—Typical ion currents of the species released during warming up of the irradiated ice samples.

TABLE 2

NUMBERS OF MOLECULES (N) OF H_2, O_2, AND H_2O_2 PRODUCED INSIDE CUBIC CRYSTALLINE WATER ICE AT DIFFERENT TEMPERATURES AND IRRADIATION CURRENTS

	10 nA		100 nA		1000 nA		10,000 nA	
MOLECULE	N	%	N	%	N	%	N	%
H_2O	6.70×10^{17}	100	6.70×10^{17}	100	6.70×10^{17}	100	6.70×10^{17}	100
				10 K				
O_2	>0	>0	$>3.11 \times 10^{13}$	>0.0046	$>1.29 \times 10^{14}$	>0.019	$>1.71 \times 10^{14}$	>0.026
H_2O_2	$>6.83 \times 10^{13}$	>0.01	$>1.28 \times 10^{15}$	>0.19	$>1.85 \times 10^{15}$	>0.28	$>1.89 \times 10^{15}$	>0.28
H_2	3.30×10^{15}	0.5	1.35×10^{16}	2.0	2.10×10^{16}	3.1	2.79×10^{16}	4.2
H_2O_2(FTIR)[a]	...	...	1.5×10^{15}	0.2	4.3×10^{15}	0.6	1.1×10^{16}	1.6
				40 K				
O_2	>0	>0	>0	>0	$>1.02 \times 10^{13}$	>0.0015	$>4.77 \times 10^{13}$	>0.0072
H_2O_2	$>4.43 \times 10^{13}$	>0.0067	$>4.74 \times 10^{13}$	>0.0070	$>7.10 \times 10^{14}$	>0.11	$>1.31 \times 10^{15}$	>0.20
H_2	2.25×10^{15}	0.33	2.41×10^{15}	0.35	8.02×10^{15}	1.2	2.13×10^{16}	3.1
H_2O_2(FTIR)[a]	...	...	...	...	2.2×10^{15}	0.3	7.8×10^{15}	1.2
				60 K				
O_2	>0	>0	>0	>0	>0	>0	>0	>0
H_2O_2	$>4.54 \times 10^{12}$	>0.00069	$>2.03 \times 10^{13}$	>0.0030	$>3.52 \times 10^{13}$	>0.0052	$>6.84 \times 10^{13}$	>0.010
H_2	7.97×10^{14}	0.12	1.22×10^{15}	0.18	2.32×10^{15}	0.35	8.38×10^{15}	1.3
H_2O_2(FTIR)[a]	...	...	...	...	1.9×10^{15}	0.3	2.8×10^{15}	0.4
				90 K				
O_2	>0	>0	>0	>0	>0	>0	>0	>0
H_2O_2	>0	>0	$>2.61 \times 10^{13}$	>0.0039	$>5.53 \times 10^{13}$	>0.0083	$>2.91 \times 10^{13}$	>0.0043
H_2	2.37×10^{14}	0.035	5.20×10^{14}	0.078	1.90×10^{15}	0.28	7.66×10^{15}	1.1
H_2O_2(FTIR)[a]	...	...	...	...	2.0×10^{14}	0.03	2.2×10^{14}	0.03

NOTE.—For comparison, the number of water molecules in the original sample and the relative conversion in percent are also compiled.

[a] Estimated from the IR absorption.

to the samples irradiated at 12, 40, 60, and 90 K, respectively. As mentioned in our previous paper (Zheng et al. 2006), H_2, O_2, and H_2O_2 were generated and trapped inside the water ice irradiated at 12 K. These molecules were released at 90–140 K (H_2), 147–151 K (O_2), and 160–180 K (H_2O_2) upon warming. The molecular hydrogen peak centered at 19 K results from residual molecular hydrogen adsorbed on the surface of the water ice. The broad H_2 and O_2 peaks at 140–175 K originated from the dissociative ionization of H_2O in the electron-impact ionizer of the mass spectrometer. In the samples irradiated at 40, 60, and 90 K, we also detected H_2 and H_2O_2 generated during the radiation exposure. In the 40 K experiment, we were also able to detect molecular oxygen (O_2). However, no molecular oxygen could be identified in the samples irradiated at 60 and 90 K. The yields, and hence the production rates, of H_2, O_2, and H_2O_2 in the irradiated water ice at distinct temperatures with different irradiation currents are summarized in Table 2. Here, the production rates of O_2 and H_2O_2 are the minimal values as described previously. The quantities of those products versus electron current at different temperatures are plotted in Figure 4. Similar to the temporal evolution of H_2O_2 column density, the relation between the product quantities and the electron current can be fitted by equation (2):

$$N(i) = a\left(1 - e^{-ki}\right), \tag{2}$$

where i is the irradiating electron current, $N(i)$ is the number of H_2, O_2, or H_2O_2 molecules generated by irradiation at electron current i, and a and k are constants. The parameters of the fits are shown in Table 3. The fits for the O_2 and H_2O_2 at 60 and 90 K are unavailable because their intensities are too low. Overall, the results from the mass spectrometry show that the production rates of H_2, O_2, and H_2O_2 decrease as the temperature increases from 12 to 90 K. This is also consistent with the results of the hydrogen peroxide development monitored via IR spectroscopy. Note that we also monitored the fragments of those molecules, such as OH, H, O, and HO_2 during irradiation and warming up. The mass spectral profiles of those fragments were similar to their parent molecules, and their intensities were a few percent of their parent molecules, which indicates that most of them were from ionization dissociation of the parent molecules inside our mass spectrometer (Zheng et al. 2006). Therefore, they are not discussed here.

It is worth mentioning that our mass spectrometer has a higher sensitivity than the IR spectrometer. The mass spectrometer was able to detect the hydrogen peroxide (H_2O_2) formed in the samples irradiated with 100 nA electron current at 40, 60, and 90 K, while the IR spectrometer could not. However, we have to keep in mind that the thermal processing of the samples after the irradiation can alter the sample composition. For instance, two hydroxyl (OH) radicals can recombine in a diffusion-limited reaction to form hydrogen peroxide upon warming the irradiated sample. Also, the mass spectrometer can monitor the IR-inactive molecules such as H_2 and O_2. On the other hand, the IR spectroscopy detected the newly formed H_2O_2 inside the ices in real time online and in situ during irradiation, whereas the mass spectrometry can only monitor the H_2O_2 until it was released into the gas phase during the warming up. Therefore, the combination of both techniques is quite important to get a complete

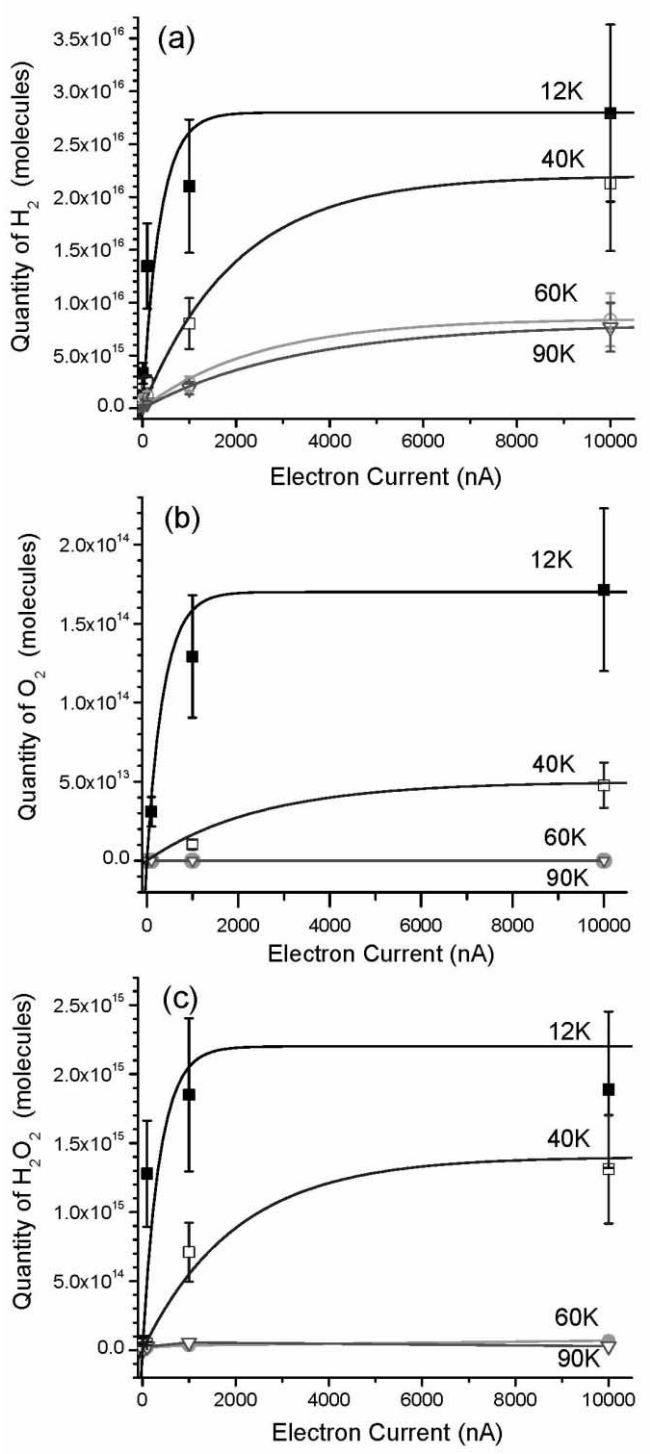

FIG. 4.—Yields of H_2 (*a*), O_2 (*b*), and H_2O_2 (*c*) vs. electron currents at different temperatures.

understanding of the underlying chemical processing of the ice samples.

4. DISCUSSION

The experiments clearly show that the amounts of H_2, O_2, and H_2O_2 produced inside the ice decrease as the irradiation temperature increases. It is also interesting that the H_2 can still be generated and trapped inside the water ice when the irradiation experiments were conducted at a temperature as high as 90 K. We also monitored the mass spectra of H_2, O_2, H_2O_2, and their fragments H, O, and OH during the irradiation. As in Zheng et al. (2006), we saw negligible amounts of products and fragments released into the gas phase during the irradiation of water ices at 12, 40, 60, and 90 K with different electron currents (10, 100, and 1000 nA). For the 10,000 nA experiments, we did see more products and fragments released during irradiation. However, the integrals of mass peaks show that the products and their fragments released into the gas phase do not have a temperature dependence. The products released into the gas phase during the irradiation were much less than the products trapped inside the water ice.

Our results are different from some previous sputtering experiments of water (or D_2O) ice conducted in the 1980s (Brown et al. 1982). Those experiments show that there were significant numbers of molecules released (sputtered) from ice into the gas phase during irradiation, and the sputtering yields of $H_2(D_2)$ and O_2 increased with increasing temperature. However, we saw a large flux of products in the gas phase during irradiation only when the electron flux was very high, i.e., in the 10,000 nA experiments (the electron flux is $\sim 3 \times 10^{13}$ electrons cm^{-2} s^{-1}). Even so, the flux of products released (sputtered) during irradiation shows no temperature dependence in the 10,000 nA experiments. Brown et al. (1982) used 1.5 MeV He^+ in the sputtering experiments. The difference between the previous experiments and our experiment might come from several things, such as different particles (electrons, for instance, do not sputter) used for irradiation, different irradiation fluxes, or different vacuum background pressures.

Brown et al. (1982) mentioned that the D_2 and O_2 yields contributed to the large increase in erosion at temperatures above 110 K. A more recent paper (Baragiola et al. 2003) shows that the total sputtering yield is constant below 60–100 K and then rises strongly due to the temperature-dependent H_2 and O_2 emission. Recently, Petrik et al. (2006) showed that the O_2 sputtering yield at steady state is relatively low and nearly constant for temperatures below ~80 K. Those results indicate the temperature dependence of $H_2(D_2)$ and O_2 sputtering yields is not very strong at lower temperatures. Our experiments were between 12 and 90 K.

Orlando & Sieger (2003) also conducted experiments to study the production of O_2 in D_2O ice by 5–100 eV electrons. They also see an increase of the O_2 production rate with temperature.

TABLE 3
BEST FITS OF THE GRAPHS SHOWN IN FIG. 4 USING EQ. (2)

	12 K		40 K		60 K		90 K	
MOLECULE	*a* (molecules)	*k* (10^{-3} nA^{-1})	*a* (molecules)	*k* (10^{-3} nA^{-1})	*a* (molecules)	*k* (10^{-3} nA^{-1})	*a* (molecules)	*k* (10^{-3} nA^{-1})
H_2	$2.8 \pm 0.9 \times 10^{16}$	2.7 ± 0.4	$2.2 \pm 0.7 \times 10^{16}$	0.5 ± 0.2	$0.85 \pm 0.3 \times 10^{16}$	0.4 ± 0.2	$0.8 \pm 0.3 \times 10^{16}$	0.3 ± 0.2
O_2	$1.7 \pm 0.6 \times 10^{14}$	2.7 ± 0.4	$0.5 \pm 0.2 \times 10^{14}$	0.4 ± 0.2	...	...	...	...
H_2O_2	$2.2 \pm 0.7 \times 10^{15}$	2.7 ± 0.4	$1.4 \pm 0.5 \times 10^{15}$	0.5 ± 0.2	...	...	...	...

The lower energy electrons mainly interact with surface layers of the water ice since they have a different stopping power from the 5 keV electrons used in our experiments. The electron flux in their experiments is $\sim 6 \times 10^{13}$ electrons cm^{-2} s^{-1}, which is about 2 times that of the 10,000 nA experiments in our case. Therefore, we are expecting more products to be released into the gas phase in their experiments. They used temperature-programmed desorption at 8 K $minute^{-1}$. In our experiment, we kept the temperature constant (0 K $minute^{-1}$) during irradiation (180 minutes), monitored the products released into the gas during irradiation, then stopped irradiation, and warmed up the samples at 0.5 K $minute^{-1}$ to allow the trapped products to be released into the gas phase. The different heating rates might also contribute to the difference between their experiments and our experiments.

There are at least four papers that discuss the temperature-dependent production of H_2O_2 in irradiated water ice. Moore & Hudson (2000) investigated the formation of hydrogen peroxide (H_2O_2) in water ice by proton (0.8 MeV) irradiation at 16 and 80 K. Although H_2O_2 was detected by IR absorption spectroscopy at 16 K, it was undetectable at 80 K. Gomis et al. (2004b) found a higher H_2O_2 production rate at 77 K than at 16 K in water ice irradiated with C^+ (30 keV), H^+ (30 keV), and O^+ (30 keV), and no difference between 77 and 16 K for the ice irradiated with N^+ (30 keV) and Ar^+ (30 keV). However, in a later paper (Gomis et al. 2004a) about water ice irradiation with H^+ (200 keV), He^+ (200 keV), and Ar^{++} (400 keV), they found a lower H_2O_2 production rate at high temperature. The irradiation experiments conducted by Loeffler et al. (2006) with Ar^+ (50–100 keV) and H^+ (100 keV) between 20–120 K also show a lower H_2O_2 yield at higher temperature. Our results agree with the literature except for Gomis et al. (2004b).

Our previous radiation exposures of crystalline water ices by 5 keV electrons at 12 K showed that the temporal profile of the hydrogen peroxide formation follows pseudo-first-order kinetics (Zheng et al. 2006). Two reaction mechanisms were proposed to account for this finding. First, the unimolecular decomposition of the water molecule and cleavage of the oxygen-hydrogen single bond can lead to the formation of a hydroxyl radical [$OH(X^2\Pi_\Omega)$] plus atomic hydrogen (eq. [3]) in an endoergic reaction (466.1 kJ mol^{-1}). Two hydroxyl radicals can recombine barrierlessly in an exoergic reaction ($\Delta_R G = -174.0$ kJ mol^{-1}) to yield a hydrogen peroxide molecule (eq. [4]). Since the hydroxyl radical is immobile at 12 K, this radical-radical recombination is limited to *neighboring* sites within a matrix cage in which both radicals have the proper *recombination geometry* (eq. [5]). Second, a water molecule was suggested to fragment via emission of electronically excited atomic oxygen (eq. [6]). The latter can react without an entrance barrier either via insertion or through a short-lived oxywater intermediate that rearranges via hydrogen migration to the hydrogen peroxide molecule (eq. [7]). If this reaction sequence happens in a matrix cage, reactions (6) and (7) can be combined to account for the experimentally observed pseudo-first-order kinetics. The reactions are as follows:

$$H_2O(X^1A_1) \rightarrow H(^2S_{1/2}) + OH(X^2\Pi_\Omega), \quad (3)$$

$$2OH(X^2\Pi_\Omega) \rightarrow H_2O_2(X^1A), \quad (4)$$

$$[(H_2O(X^1A_1))_2] \rightarrow [H(^2S_{1/2})..HO(X^2\Pi_\Omega)..OH(X^2\Pi_\Omega)..H(^2S_{1/2})] \rightarrow H_2O_2(X^1A) + 2H(^2S_{1/2}), \quad (5)$$

$$H_2O(X^1A_1) \rightarrow O(^1D) + H_2(X^1\Sigma_g^+), \quad (6)$$

$$O(^1D) + H_2O(X^1A_1) \rightarrow H_2O_2(X^1A), \quad (7)$$

$$O(^1D) + H_2O(X^1A_1) \rightarrow [OOH_2(X^1A)] \rightarrow H_2O_2(X^1A), \quad (8)$$

$$[(H_2O(X^1A_1))_2] \rightarrow [H_2(X^1\Sigma_g^+)...H_2O(X^1A_1)...O(^1D)] \rightarrow H_2(X^1\Sigma_g^+) + H_2O_2(X^1A), \quad (9)$$

$$[(H_2O(X^1A_1))_2] \rightarrow [H_2(X^1\Sigma_g^+)...H_2O(X^1A_1)...O(^1D)] \rightarrow [H_2(X^1\Sigma_g^+)...H_2OO(X^1A)] \rightarrow H_2(X^1\Sigma_g^+) + H_2O_2(X^1A). \quad (10)$$

How can these reaction mechanisms account for the temperature dependence of the observed production rates of, for instance, hydrogen peroxide? Two reaction scenarios might explain the experimental findings. First, as the temperature increases, the primary fragments of the oxygen-hydrogen bond ruptures, i.e., atomic hydrogen, hydroxyl radical, and atomic oxygen, easily diffuse at elevated temperatures and can be released into the gas phase; this open system scenario would exclude these open shell species from the synthesis of hydrogen peroxide. However, since we monitored the gas phase with a mass spectrometer and no enhanced emission of these species was observed, this possibility can be excluded.

Second, we have to keep in mind that the enhanced temperature can increase the diffusion coefficient D of the atoms (oxygen, hydrogen) and of the hydroxyl (OH) radical significantly (eq. [11]) (Hori & Hondoh 2003),

$$D = D_0 e^{-\Delta E_{\text{barrier}}/kT}. \quad (11)$$

Here, D_0 represents the preexponential factor, k represents the Boltzmann constant, T represents the temperature, and $\Delta E_{\text{barrier}}$ represents the barrier the species has to overcome to "move" from one lattice site to the other. Considering, for instance, the diffusion of a hydrogen atom and a hydrogen molecule in hexagonal water ice, $\Delta E_{\text{barrier}}$ was determined to be 13 kJ mol^{-1} and about 1 kJ mol^{-1}, respectively (Strauss et al. 1994). Therefore, an increase of the temperature from 12 to 90 K enhances the diffusion coefficients of the thermalized hydrogen atoms and hydrogen molecules by 60 and 4 orders of magnitude, respectively. These estimates verify the strong influence of the ice temperature on the diffusion coefficient of the hydrogen atom and molecular hydrogen. Considering equation (3), we can therefore expect that *thermalized* hydrogen atoms in a matrix cage can—due to their enhanced diffusion coefficients at elevated temperatures—recombine with the hydroxyl radical to "recycle" the water molecule. This would reduce the concentration of the hydroxyl radical and result in a diminished formation of hydrogen peroxide molecules. On the other hand, electronically excited oxygen atoms generated via equation (6) can only recycle a water molecule if their lifetime in the ice is longer than the timescale needed to diffuse back to the hydrogen molecule, i.e., the reverse reaction (6) to recover a water molecule. Due to the lower mass of 1 versus 16 amu, the lighter hydrogen atom should diffuse faster than the oxygen atom; therefore, an elevated temperature should have a pronounced effect on the recycling of water via the reverse reaction (3).

The preferential back-reaction of atomic hydrogen with the hydroxyl radical also gains support from the temperature-dependent

yields of the hydrogen molecule. Note that enhanced mobility of the hydrogen atom could also result in an increase of the formation rates of molecular hydrogen as the temperature rises. However, this was not observed experimentally. Therefore, our data suggest that the mobile hydrogen atom rather recombines in the matrix cage with the hydroxyl radical than diffusing outside the matrix cage and reacting with a second hydrogen atom to form molecular hydrogen.

Another possibility might be the destruction of H_2O_2 at higher temperature as suggested by Moore & Hudson (2000). The OH radicals from H_2O_2 destruction react with the newly formed hydrogen atoms or molecules and therefore reduce the amount of both H_2O_2 and H_2. Since H_2O_2 might be one of the major precursors of O_2, this could also reduce the production of O_2. Note that this still supports the idea of OH and H recombination because hydrogen molecules are not as reactive as hydrogen atoms. Considering the low concentration of H_2O_2 relative to H_2O, we are expecting that most OH radicals come from the electron destruction of water molecules. Although the destruction of H_2O_2 can reduce the amount of products, the lower production rates at higher temperatures are mainly due to OH and H recombination.

5. ASTROPHYSICAL IMPLICATIONS

Absorption features of hydrogen peroxide have been identified in the IR and UV regime on Europa at concentrations of about $0.13\% \pm 0.07\%$ relative to water (Carlson et al. 1999). Hendrix et al. (1999) reported the existence of hydrogen peroxide on the surfaces of Europa, Ganymede, and Callisto with concentrations of about 0.3%. The authors speculate that hydrogen peroxide originates from an irradiation of water ice by energetic particles in those systems. Our experiments conducted at 90 K—a temperature characteristic of the conditions on Europa, Ganymede, and Callisto—might be able to simulate the chemical processing of water ices on the Galilean satellites. In our experiments, the incident energy flux of the irradiation at 1000 nA electron current for 180 minutes is about 1.67×10^{20} eV cm^{-2}. That corresponds to an energy deposition of about 1 month on Europa (7.8×10^{13} eV cm^{-2} s^{-1}), 1 yr on Ganymede's polar cap (5.4×10^{12} eV cm^{-2} s^{-1}), 20 yr on Ganymede's equator (2.6×10^{11} eV cm^{-2} s^{-1}), and 25 yr on Callisto (2.2×10^{11} eV cm^{-2} s^{-1}) (Cooper et al. 2001). In the 90 K experiment, the H_2O_2 concentration measured from the IR spectrum is about 0.03%. This value is about 4 times lower than the concentration of H_2O_2 on Europa measured by Carlson et al. (1999) and 10 times lower than those reported by Hendrix et al. (1999). We believe the concentration measured from our IR spectrum has been underestimated due to the overlapping between the H_2O_2 band and H_2O bands. As our mass spectrometer has better sensitivity, we tried to estimate the H_2O_2 concentration based on the amount of molecular hydrogen detected with our mass spectrometer. Since H_2, O_2, and H_2O_2 all come from water molecules—according to stoichiometry—equation (12) holds. Here, $[H_2]$, $[O_2]$, and $[H_2O_2]$ represent the concentrations of H_2, O_2, and H_2O_2, respectively. A rearrangement of equation (12) yields equation (13):

$$(2[H_2] + 2[H_2O_2]):(2[H_2O_2] + 2[O_2]) = 2:1, \quad (12)$$

$$[H_2] - [H_2O_2] = 2[O_2]. \quad (13)$$

From Table 2, we can conclude that the quantity of O_2 is much lower than that of H_2O_2. So it is easy to see that the concentration of H_2O_2 is about the same as that of H_2. At least, they should be the same order of magnitude. In Table 2 at an irradiation current of 1000 nA at 90 K, the concentration of molecular hydrogen and hence of hydrogen peroxide is about 0.28% relative to water by molecule number. This number is close to the number measured from the UV spectra of Europa by Hendrix et al. (1999). Yet we cannot claim that our experiments exactly reproduced the conditions on Europa or the other Galilean satellites because our IR spectrum is not very similar to the IR spectrum of Europa. Note that the IR spectra can be influenced by many different things, such as ice granule size, impurities inside the ice, etc. The compositions of the ice on the Galilean satellites probably are much more complicated than those in our experiments. Therefore, we can only say the concentration of H_2O_2 in our 90 K experiments is in the same order of magnitude as those observed on the Galilean satellites.

Since the production rates of H_2, O_2, and H_2O_2 decrease with increasing temperature, we predict that the concentrations of those species are higher in the low-temperature objects; therefore, we expect more H_2, O_2, and H_2O_2 on the surfaces of Kuiper Belt objects than on the comets and icy satellites at a comparable energy deposition. This underlines the necessity to provide temperature-dependent formation rates of astrophysically important molecules in processed ice samples. As a matter of fact, the diffusion coefficient of atoms, radicals, and molecular species such as hydrogen and oxygen was also predicted to depend on the crystal structure, i.e., crystalline versus amorphous water (Hori & Hondoh 2003). Therefore, it is also important to investigate the effects of the crystal structure on the formation rates of hydrogen, oxygen, and hydrogen peroxide at distinct temperatures.

This work was financed by the NASA Astrobiology Institute under cooperative agreement NNA04CC08A at the University of Hawaii at Manoa (W. Z., D. J., and R. I. K.) and by the US National Science Foundation (NSF; AST 05-07763; D. J., R. I. K.). We are grateful to Ed Kawamura (University of Hawaii at Manoa, Department of Chemistry) for his electrical work.

REFERENCES

Bahr, D. A., Fama, M., Vidal, R. A., & Baragiola, R. A. 2001, J. Geophys. Res., 106, 33285
Baragiola, R. A. 2003, Planet. Space Sci., 51, 953
Baragiola, R. A., Loeffler, M. J., Raut, U., Vidal, R. A., & Wilson, C. D. 2005, Radiat. Phys. Chem., 72, 187
Baragiola, R. A., Vidal, R. A., Svendsen, W., Schou, J., Shi, M., Bahr, D. A., & Atteberrry, C. L. 2003, Nucl. Instrum. Methods Phys. Res. B, 209, 294
Bennett, C. J., Jamieson, C., Mebel, A. M., & Kaiser, R. I. 2004, Phys. Chem. Chem. Phys., 6, 735
Bennett, C. J., Jamieson, C. S., Osamura, Y., & Kaiser, R. I. 2005, ApJ, 624, 1097
Brown, R. H., & Cruikshank, D. P. 1997, Annu. Rev. Earth Planet. Sci., 25, 243
Brown, W. L., et al. 1982, Nucl. Instrum. Methods, 198, 1
Calvin, W. M., Clark, R. N., Brown, R. H., & Spencer, J. R. 1995, J. Geophys. Res., 100, 19041
Carlson, R. W., et al. 1999, Science, 283, 2062
Cecchi-Pestellini, C., Aiello, S., & Barsella, B. 1995, MNRAS, 274, 134
Cesarsky, C. J., & Volk, H. J. 1978, A&A, 70, 367
Clayton, D. D., & Jin, L. 1995, ApJ, 451, 681
Cooper, J. F., Christian, E. R., Richardson, J. D., & Wang, C. 2003, Earth Moon Planets, 92, 261
Cooper, J. F., Johnson, R. E., Mauk, B. H., Garrett, H. B., & Gehrels, N. 2001, Icarus, 149, 133
Davies, J. K., Roush, T. L., Cruikshank, D. P., Bartholomew, M. J., Geballe, T. R., Owen, T., & de Bergh, C. 1997, Icarus, 127, 238

Festou, M., Keller, H. U., & Weaver, H. A., eds. 2004, Comets II (Tucson: Univ. Arizona Press)
Flasar, F. M., et al. 2005, Science, 307, 1247
Gomis, O., Leto, G., & Strazzulla, G. 2004a, A&A, 420, 405
Gomis, O., Satorre, M. A., Strazzulla, G., & Leto, G. 2004b, Planet. Space Sci., 52, 371
Greenberg, J. M., van de Bult, C. E. P. M., & Allamandola, L. J. 1983, J. Phys. Chem., 87, 4243
Hanel, R., et al. 1979, Science, 206, 952
———. 1982, Science, 215, 544
Hendrix, A. R., Barth, C. A., Stewart, A. I. F., Hord, C. W., & Lane, A. L. 1999, Lunar Planet. Sci. Conf., 30, 2043
Hori, A., & Hondoh, T. 2003, Canadian J. Phys., 81, 251
Jamieson, C. S., Bennett, C. J., Mebel, A. M., & Kaiser, R. I. 2005, ApJ, 624, 436
Jewitt, D., & Luu, J. 1993, Nature, 362, 730
———. 2004, Nature, 432, 731
Johnson, R. E., Cooper, P. D., Quickenden, T. I., Grieves, G. A., & Orlando, T. M. 2005, J. Chem. Phys., 123, 184715
Johnson, R. E., & Quickenden, T. I. 1997, J. Geophys. Res., 102, 10985
Kaiser, R. I. 2002, Chem. Rev., 102, 1309
Kruegel, E., & Walmsley, C. M. 1984, A&A, 130, 5
Loeffler, M. J., & Baragiola, R. A. 2005, Geophys. Res. Lett., 32, L17202
Loeffler, M. J., Raut, U., Vidal, R. A., Baragiola, R. A., & Carlson, R. W. 2006, Icarus, 180, 265
Moore, M. H., & Hudson, R. L. 2000, Icarus, 145, 282
Orlando, T. M., & Sieger, M. T. 2003, Surface Sci., 528, 1
Petrik, N. G., Kavetsky, A. G., & Kimmel, G. A. 2006, J. Phys. Chem. B, 110, 2723
Sicardy, B. 2005, Space Sci. Rev., 116, 457
Spencer, J. R., Tamppari, L. K., Martin, T. Z., & Travis, L. D. 1999, Science, 284, 1514
Strauss, H. L., Chen, Z., & Loong, C. K. 1994, J. Chem. Phys., 101, 7177
Zheng, W., Jewitt, D., & Kaiser, R. I. 2006, ApJ, 639, 534